A floating self-propelling liquid marble containing aqueous ethanol solutions

Author

Ooi, Chin Hong, Anh, Van Nguyen, Evans, Geoffrey M, Gendelman, Oleg, Bormashenko, Edward, Nam-Trung, Nguyen

Published

2015

Journal Title

RSC Advances

Version

Accepted Manuscript (AM)

DOI

10.1039/c5ra23946j

Cite this: DOI: 10.1039/x0xx00000x

Floating self-propelling liquid marble containing aqueous ethanol solutions

Chin Hong Ooi,[a] Anh Van Nguyen,[b] Geoffrey M. Evans, [c] Oleg Gendelman, [d] Edward Bormashenko,[e] Nam-Trung Nguyen,[a*]

Received 00th January 2012,
Accepted 00th January 2012

DOI: 10.1039/x0xx00000x

www.rsc.org/

A liquid marble is a droplet coated with hydrophobic particles. A floating liquid marble is a unique reactor platform for digital microfluidics. The autonomous motion of a liquid marble is of great interest for this application because of the associated chaotic mixing inside the marble. A floating object can move by itself if a gradient of surface tension is generated in the vicinity of the object. This phenomenon is known as the Marangoni solutocapillary effect. We utilized a liquid marble containing a volatile substance such as ethanol to generate the solutocapillary effect. The paper reports a qualitative study on the operation conditions of liquid marbles containing aqueous ethanol solutions in autonomous motion due to the Marangoni solutocapillary effect. We also derive the scaling laws relating the dynamic parameters of the motion to the physical properties of the system such as the effective surface tension of the marble, the viscosity and the density of the supporting liquid, the coefficient of diffusion of the ethanol vapour, the geometrical parameters of the marble, the speed, the trajectory and the lifetime of the autonomous motion. A self-driven liquid marble has the potential to serve as an effective digital microfluidic reactor for biological and biochemical applications.

1. Introduction

We recently successfully used the floating liquid marble, a liquid droplet coated with hydrophobic particles, as a bioreactor platform to grow three-dimensional (3D) cell spheroids.[1] The quality of the spheroids depend on the internal mixing process, which in turn depends on the motion of the marble over the surface of the supporting liquid. The autonomous motion of a floating object induced by the Marangoni solutocapillary effect has been studied,[2-6] especially that of a camphor boat.[7-11] Floating particles infused with volatile compounds can even be programmed to "dance"[12] or navigate in complex environments.[13] The relationship between the translational and rotational motion of a floating object to the surface tension and concentration was also investigated.[14-16] Recently, Bormashenko et al. reported the solutocapillarity driven self-propulsion of a floating marble filled with an ethanol/water mixture.[17] With the potential use of a liquid marble as a digital microfluidic reactor platform, manipulation of a liquid marble attracted great interest from the microfluidics community. A liquid marble has been manipulated on a solid surface using electrostatic[18] or magnetic[19-22] means to induce the motion.

The present paper investigates the operation parameters and dynamic characteristics of the moving, floating ethanol/water marble. We first determine the relative sizes of marbles to their respective boundaries as a condition to initiate the solutocapillary motion. Previous works indicated that a camphor boat placed inside a small boundary cannot move across the water surface. In our case, we seek to investigate and explain the threshold size with respect to the marble size and the driving force. The marble size was varied using different liquid volumes, while the driving force was controlled by different ethanol concentrations of the marble liquid. Scaling analysis was carried out to explain the relationship between the size of liquid surface and the size of the marble. Both experimental data and the scaling relationships lead to an operation map for self-propelling liquid marbles.

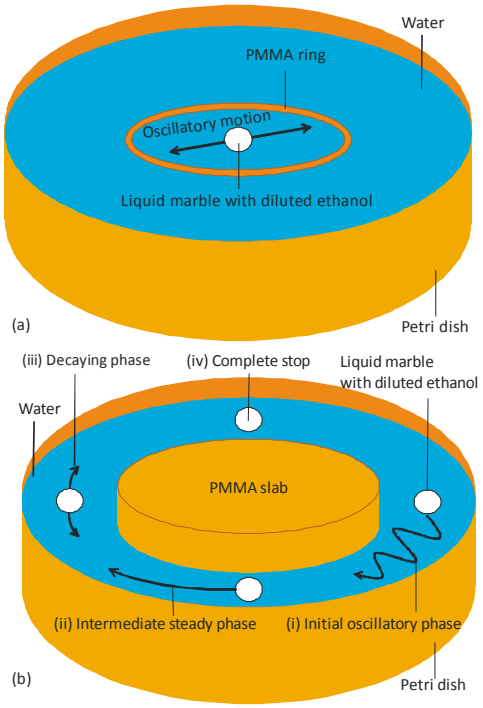

Fig. 1 Experimental setups: (a) Effect of relative boundary size: The liquid marble is placed in a PMMA ring that determines the domain of the open surface for its motion. Water from both sides of the ring is connected so that the same surface level is maintained. (b) Motion of a liquid marble on a circular channel track: The marble traverses the annular channel, starting at the right side and moving in a clockwise fashion. After several laps, the marble movement changes from an (i) oscillatory phase to (ii) a steady phase, followed by a (iii) decaying phase and (iv) a complete stop.

Next, we investigated the kinematic behaviour of a moving, floating liquid marble. The marble was placed on an air-water interface in an annular channel filled with water. The motion of the marble was analysed by digital image processing. A scaling analysis was carried out for the speed of the marble and its volume. We then compared and discussed the data obtained for the liquid marbles with those from the previous studies on camphor boats. In the camphor boat experiments, the camphor slowly lost its mass but retained its ability to release chemical reagents. In contrast, the ethanol concentration and the motion in our experiments decayed over time, due to the limited mass of ethanol as fuel available in the marbles. Therefore, the duration of the motion would be an important parameter and was investigated as well.

Figure 1 shows the schematic setup of the experiments conducted and reported in this paper. We used rings made of polymethyl methacrylate (PMMA) with different diameters to control the boundary around a floating liquid marble. After placing the marble onto the water surface within the ring, the ethanol diffuses from the marble onto the water surface. Ethanol molecules absorbed by water lower the surface tension and form a surface tension gradient in the vicinity of the marble. The gradient and the corresponding Marangoni force drive the motion of marble. The driving force for this movement is well understood and is a product of the characteristic length of the floating object and the gradient of the surface tension. The movement can then be described by the Newtonian equation as follows:

$$m\frac{d\vec{v}_{cm}}{dt} = \vec{F}_{fr} + \alpha L^2 \nabla\gamma = -\chi L\eta\vec{v}_{cm} + \alpha L^2\nabla\gamma \qquad (1)$$

where m, and v are the mass, and velocity of the centre of mass of the marble, respectively. The characteristic length L is of order of magnitude of the radius of the marble contact area. The friction force $\vec{F}_{fr}$ mainly comes from the viscous drag which is proportional to the dynamic viscosity of the supporting liquid η ,[10] α and χ are dimensionless coefficients. $\chi \approx 10$ represents the friction factor, which is 3π in case of Stokes drag of a solid spherein an unbounded fluid. The second term on the right side of equation (1) represents the Marangoni force, which is a function of the gradient of the ethanol concentration c on the water surface.

Previous experiments of Hayashima et al.[10] indicated that the motion of a camphor scraping on the water surface is affected by the sublimation and dissolution rate of camphor, and the length of the water chamber. Changing one of these parameters may result in no motion, oscillatory motion or collisions with the chamber wall. These previous experiments involved the variation of the container size. The water temperature was used to control the sublimation and dissolution rate of camphor in water. Nagayama et al.[23] also reported a numerical simulation based on the Newtonian equation of motion and reaction-diffusion equations.

In most applications with liquid marbles the temperature of the carrier liquid is considered as constant. The volume of the liquid marble is often the varying independent parameter. Therefore, we focus on the effects of ethanol concentration, the size of the liquid marble and the size of the open surface boundary. A circular chamber was used in the experiments to reduce the spatial dimension to a single radial distance.

The diffusion of ethanol is governed by the reaction-diffusion equation[14]

$$\frac{\partial c}{\partial t} = D\frac{\partial^2 c}{\partial x^2} - kc + f(x,r,S) \qquad (2)$$

where c is the ethanol concentration, D is the diffusion coefficient, k is the combined evaporation and dissolution rate of ethanol at the water surface, x and r are the position and nominal radius of the marble respectively, S is the supply rate of ethanol from the liquid marble to the water surface. The term f indicates that the driving Marangoni force of the floating liquid marble can be increased by increasing the supply rates S. Increasing the concentration of ethanol in the marble can increase the supply rate.

If the size of the marble increases while the concentration of ethanol remains constant, the motion is affected by two competing factors. First, the larger contact surface between the marble and the open surface will increase the friction term in equation (1). Conversely, the larger contact surface increases the supply of ethanol to the water surface as well as a larger characteristic length, creating a larger concentration gradient and driving Marangoni force.

2. Materials and methods

Laboratory-grade pure ethanol (Chem-Supply) was diluted with deionized (DI) water in different ratios. For liquid marble preparation, the loose polytetrafluoroethylene (PTFE, Sigma-Aldrich®) particles used had a nominal diameter of 1 µm. Diluted ethanol was dispensed onto the PTFE powder bed and rolled around until the droplet was completely covered and the marble was formed. A pipette (Thermo Scientific Finnpipette 4500, 0.5-10µL) was used as the dispenser for accurate volume control. The liquid marble was then rolled around on a clean stainless steel spoon to dislodge excess powder on the marble shell. The effective surface tension of the liquid marble was estimated with the puddle height method.[24] The side view of the sessile liquid marble was imaged with a digital camera and the maximum height was recorded. The experiment was conducted in a controlled laboratory environment with a temperature of 19 °C and a relative humidity of 62 %.

In the experiment shown in Fig. 1(a) the Petri-dish was partially filled with DI water. Laser cutter machined PMMA rings with different diameters were used for the experiments. The ring diameter ranged from 15 to 40 mm in 2.5 mm size increment. The ring was then placed in the Petri-dish to act as the boundary for the floating liquid marble. More water was added until the water level approached the top of the ring. The prepared marble was then carefully placed inside the ring. The marble movement was then able to be observed. The experiment started with placing the largest ring (40 mm) on the Petri dish. If the liquid marble was able to move the next ring size was subsequently tested. If the marble stopped immediately upon the placement of the ring the preceded ring size was taken as the critical minimum ring diameter that allowed the marble to move. This procedure was repeated for the different marble volumes and ethanol concentrations.

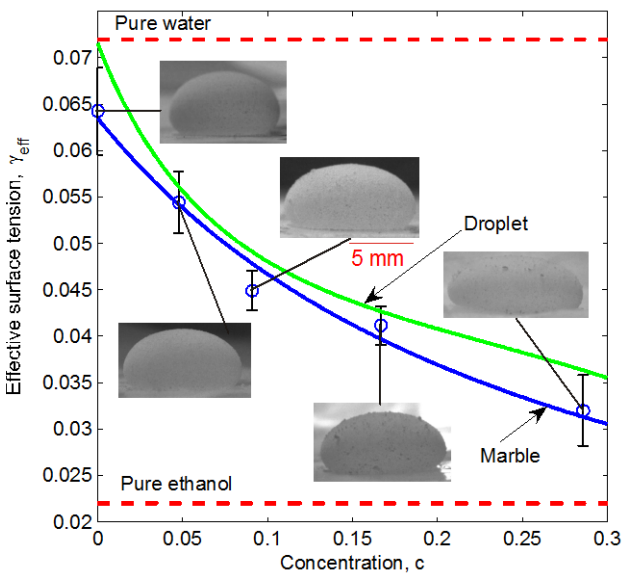

Fig. 2 Effective surface tension of the liquid marble and liquid droplet[1] versus the volume concentration of ethanol. The insets show the shape of the liquid marble with increasing ethanol concentration. The top and bottom dashed red lines show surface tension of pure water (0.0715 N/m) and ethanol (0.0223 N/m), respectively.

In the experiment shown in Fig. 1(b), a circular PMMA slab of 70-mm diameter was fixed at the centre of the petri dish of 140-mm diameter to create an annular channel with a width of 35mm. The channel was then filled with water. The prepared marble was subsequently placed in the water channel and the movement was recorded from above with a digital. The video was processed to extract the centroid position of the marble from individual frames using Matlab (Mathworks). With the known frame rate of the video, the position data was further evaluated to obtain the velocity and acceleration data of the marble.

3. Results and discussions

3.1. Effective surface tension of floating liquid marble

Measurement of the effective surface tension of the liquid marble is a challenging task. The effective surface tension of a liquid marble is known to depend on the volume and the marble preparation conditions.[25] Additionally, a liquid marble that floats on a liquid carrier deforms, and a layer of coating is sandwiched between the marble liquid and the carrier liquid.[26] This effect influences the distribution of coating particles on the surface of the liquid marble and consequently impacts its effective surface tension. Various methods have been utilised to measure the effective surface tension.[24, 27-29] However, all of these methods apply to a sessile liquid marble resting on a solid surface. In our case, the marbles containing aqueous alcohol solutions moved rapidly across the carrier surface making accurate measurement extremely challenging. For this reason, we used the puddle height method[24] to approximate the effective surface tension of the floating liquid marble. Measuring the puddle height, the effective surface tension was estimated as $\gamma_{eff}=h^2\rho g/4$, where h is the maximum puddle height, ρ is the density of the ethanol-water mixture and g is the gravitational acceleration.

Measurement of the effective surface tension was carried out to determine the corresponding Bond number for the dimensionless analysis. Bond number can be defined as $Bo = \rho g r^2/\gamma_{eff}$ where r is the radius of the non-deformed spherical marble. As expected, increasing ethanol concentration lowers the surface tension of the liquid marble, Fig. 2. The result is similar to that of a previous study regarding surface tension and ethanol concentration which does not involve a

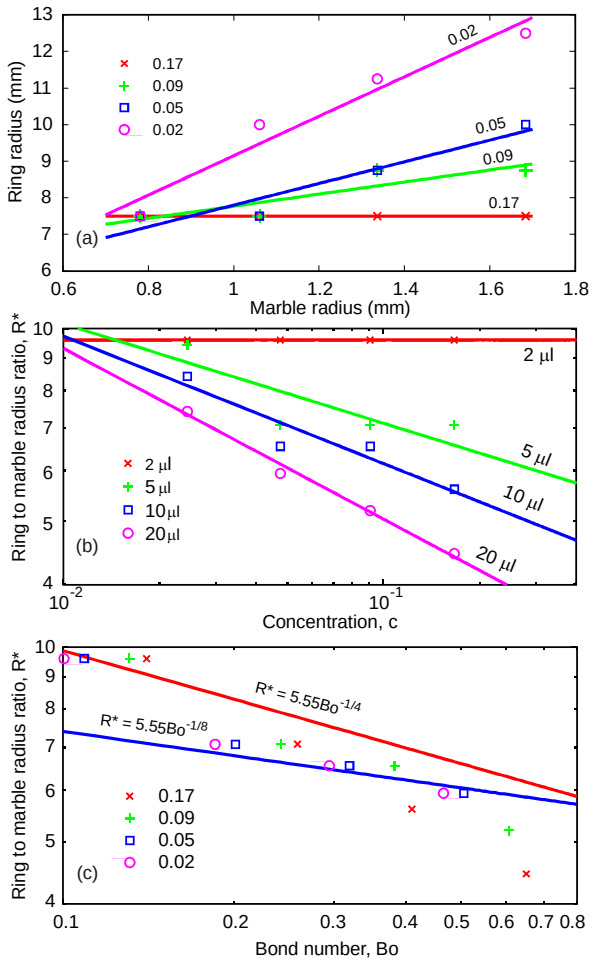

Fig. 3 Condition for self-driving liquid marbles: (a) Minimum (critical) ring radius enabling marble motion versus the diameter of the non-deformed marble for different volume concentrations of ethanol. (b) Radius ratio between the ring and the marble diameter versus volume concentration of ethanol for different marble volumes. (c) Diameter ratio between the ring and the marble diameter versus Bond number for different volume concentration of ethanol.

sessile droplet. The fitting line has the form of $\gamma_{eff}=\gamma/(1+ac)$ where a is a constant and c is the volume concentration. The trend in Fig. 2 is similar to previous studies on the correlation between the effective surface tension and the volume concentration.[10]

3.2 Marble size relative to working area

Figure 3(a) shows the minimum or critical ring radius that allows the movement of a floating liquid marble versus the radius of the non-deformed marble for different ethanol volume concentrations. The minimum radius was identified when placing the ring on the water stopped the self-propulsion of the liquid marble. The marble either ceases to move almost instantly or wobble about within the ring for a short time. We only consider the translational self-propulsion as the movement, and observed that threshold values of the ring size and the ethanol concentration exist for self-propulsion of the marble. These values vary with marble size, and at the highest volume concentration (c = 0.17), the marbles of all investigated volumes move in the smallest 15-mm ring.

Figure 3(a) indicates that the minimum ring size enabling the marble movement increases with increasing marble volume and increasing volume concentration of ethanol. The increasing ethanol concentration increases the concentration gradient and consequently the driving force of the marble. It is plausible to introduce the dimensionless ratio $R^*=R/(r)$ for the interpretation of the results of different marble volumes, where R is the ring radius and r is the radius of the non-deformed marble.

Figure 3(b) shows the ratio R^* versus the volume concentration of ethanol, c, for different volumes. The Bond numbers in the experiments are relatively small (Bo<1), as the marble is quasi-spherical even on the water surface. Any ratio that is greater than this minimum R^* will result in marble motion, where operation region for a self-driving marble is in the upper right side above the threshold line.

Figure 3(c) shows the ring to diameter ratio R^* versus the Bond number for different volume concentrations of ethanol. The minimum ratio R^* decays with the Bond number, where a low volume concentration of ethanol causes a faster decrease of R^* with increasing Bond number. This behaviour indicates a scaling law between the R^* and Bo.

For the ethanol concentration of 0.02, the 2-µL marble holds sufficient ethanol to sustain movement for several seconds. Although the self-propulsion is observed, ethanol as fuel dissipates very quickly. Conversely, the marble with the most ethanol (20-µL marble with 0.17 volume concentration of ethanol) ceases to move relatively quickly, when it was placed in a small ring. If the ring size is smaller than a threshold, no marble movement was observed. The marble may show an overdamped oscillatory behaviour and it stops at the centre of the ring.

The characteristic time necessary for the acceleration of the marble to the steady state may be estimated from Eq. (1) as:

$$\tau_m \approx \frac{m}{\chi L \eta} = \frac{4\pi r^3 \rho}{3\chi L \eta} \qquad (3)$$

Equation (2) indicates that re-condensed ethanol will cover the ring radius R after a characteristic diffusion time, which can be estimated from the Stoke-Einstein model of diffusion as:

$$\tau_c = \frac{R^2}{2D} \qquad (4)$$

We hypothesise that the marble is able to move if it has enough time to accelerate before the uniform concentration of the ethanol inside the ring is achieved. Thus the scaling relationship for radius of the ring can be estimated from $\tau_c = \tau_m$:

$$\frac{R^2}{2D} = \frac{4\pi r^3 \rho}{3\chi L \eta} \tag{5}$$

or

$$R = \sqrt{\frac{8\pi D\rho}{3\chi\eta}\frac{r^3}{L}} \tag{6}$$

Characteristic value of the contact radius can be estimated from the scaling analysis from Aussillous and Quere for a sessile marble on a solid surface:[17]

$$L = \sqrt{2/3} r^{3/2} l^{-1/2} \text{ for } \quad >1 \tag{7}$$

and

$$L = \sqrt{2/3} r^{2} l^{-1} \text{for } \ \text{Bo} \le 1 \tag{8}$$

where $l = \sqrt{\gamma_{\text{eff}} / \rho g}$ is the capillary length. The characteristic length can be expressed in terms of Bond number as:[13]

$$L = \sqrt{2/3} r \text{Bo}^{1/4} \text{for} \text{Bo} > 1 \tag{9}$$

$$L = \sqrt{2/3} r \text{Bo}^{1/2} \quad \text{for Bo} \le 1 \tag{10}$$

Substituting (9) and (10) into (6) results in the scaling relation for the dimensionless ring ratio:

$$R^* = \frac{R}{r} = \sqrt{\frac{8}{\sqrt{6}}\frac{\pi D\rho}{\chi\eta}} \text{Bo}^{-1/8} \quad \text{for Bo} > 1 \tag{11}$$

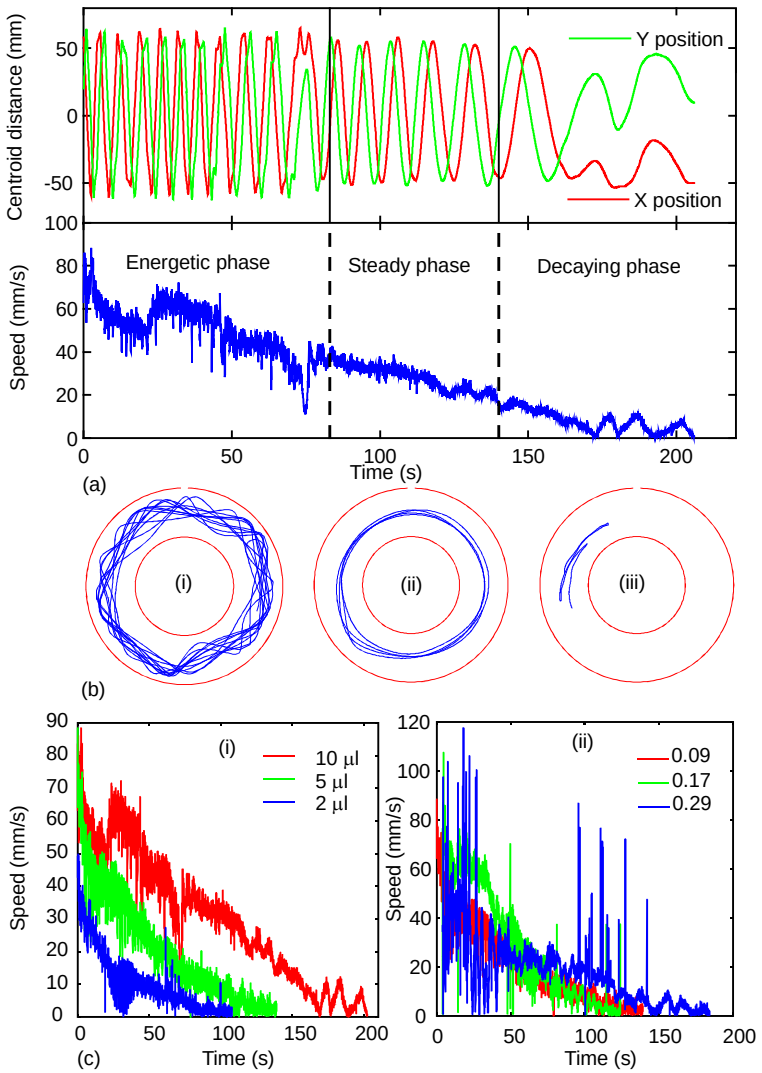

Fig. 4 Kinematic behaviour of a self-driven marble in a circular channel track: (a) Full speed and displacement profile with different phases (10 µl marble, concentration 0.09); (b) Characteristic marble paths of each phase (10 µl marble, concentration 0.09): (i) The initial oscillatory phase with wavy path (video S1). (ii) The intermediate steady phase with a well defined circular path (video S2). (iii) The decaying phase with "stop and go" behaviour (video S3). (c) Time history of the speed of floating liquid marbles in an annular channel with different (i) volumes and (ii) volume concentration of ethanol.

$$R^* = \frac{R}{r} = \sqrt{\frac{8}{\sqrt{6}}\frac{\pi D\rho}{\chi\eta}}\mathrm{Bo}^{-1/4} \text{ for } \mathrm{Bo} \le 1 \quad (12)$$

For the purpose of fitting the experimental data in Fig. 3(a), we used a diffusion coefficient in the gas phase of $D = 3\cdot 10^{-5} m^2/s$, a viscosity of $\eta = 10^{-3} Pa\cdot s$, a density $\rho = 10^3 \mathrm{kg/m}^3$ and the dimension less coefficient $\chi \approx 10$ resulting in a scaling factor of 5.55.

3.3 Kinematic behaviour

The position (*x*,y) of the marble is extracted from the recorded videos. Figure 4(a) shows the representative *x* and *y* positions of the centroid of the marble over the lifetime of the movement. The speed of the marble can be found by $v_i = \sqrt{(x_{i+1}-x_i)^2 + (y_{i+1}-y_i)^2}/\Delta t$, where *i* indicates the frame and Δt is the time between two consecutive video frames. The sinusoidal shape of the position comes from the circular trajectory of the marble in the annular water channel. The time history of the speed clearly shows three phases of the movement: the initial oscillatory phase, the intermediate steady phase and the final decaying phase. Figure 4(b) shows the typical trajectories of the marble in these three phases.

During the initial oscillatory phase the velocity of the marble has both tangential and radial components. The tangential component is not oscillatory because the marble follows the trajectory in the annular channel. In contrast, the radial motion is oscillatory because the channel is wide relative to the marble and the marble bounces from one channel side to the other. The marble was repelled by the channel wall due to a combination of the meniscus and lowered concentration gradient effect, as described in detail by Chen et al..[4]

After the oscillatory phase, the ethanol concentration decreased and the marble was less energetic. The movement became steady and the marble proceeded with several laps around the channel. In this steady phase the speed only has a tangential component. The marble was not energetic enough to induce radial oscillations. This change of movement phase has been observed in floating droplets as well.[4]

Finally, as the fuel was spent the marble became even less energetic and entered the decaying phase. Even unidirectional tangential motion became more difficult. The marble shows a "stop-and-go" behaviour. As the ethanol concentration reduced the marble no longer has enough fuel and the corresponding Marangoni force to move. Minor perturbations along the way will cause the marble to move in an unpredictable manner until it eventually ceases to move.

Eq. (1) predicts for the steady-state motion of a marble will have a velocity of:

$$v_{cm} \cong \frac{\alpha}{\chi}\frac{|\nabla\gamma|}{\eta}L \quad (13)$$

where the characteristic length *L* is of the order of magnitude of the radius of the marble contact area. Considering the scaling laws (7) and (8), relating the radius of the marble contact area *L* to the radius of non-deformed marble *r* discussed above[17], yields the weak dependence of the steady-state velocity of the marbles:

$$v_{cm} \sim L \sim r^{1.5} \sim V^{0.5}. \quad (14)$$

Therefore, for the same concentration of ethanol a smaller marble will move with a lower speed. The above scaling relationship is recognizable in Fig. 4(c).

Moreover, Figure 4(c) shows that the speed of the marble decreases almost exponentially over time. An analysis of the two governing equations (1) and (2) reveals that the solution for the instantaneous speed is complicated. The Newtonian equation of motion (1) has an inertial term on the left hand side. In previous quantitative studies on camphor boats, the mass and supply rate are assumed to be constant, since the amount of camphor loss due to sublimation is negligible throughout the duration of the experiment.[14] The supply rate of camphor is also constant because the sublimation process of a pure camphor boat does not alter its concentration.

The above assumptions are not applicable for the case of a self-driven floating marble. Although the marble coating reduces the evaporation rate of ethanol and water, the ethanol evaporation rate is significantly higher than that of water under standard temperature and pressure conditions, especially for marbles with high ethanol concentration.[30] Assuming that the ethanol-water mixture within the marble is homogenous, then the evaporation occurs throughout the entire surface of the marble. Some of the ethanol molecules eventually dissolve in the liquid carrier, whilst the rest just dissipates into the air. Therefore, the marble mass will decrease over time.

The evaporation of an ethanol-water mixture is also known to change the remaining ethanol concentration, which in turn affects the evaporation rate.[31] Thus, the concentration of ethanol is highly time dependent. Consequently, the supply rate of ethanol and the surface tension gradient across the marble are also functions of time. To the best of our knowledge, no work has been conducted to measure or model the evaporation rate of a floating liquid marble, especially with an ethanol-water mixture.

3.4 Duration of the motion

The duration of the motion of the marble relates only to the self-propulsion time span and not the total lifetime until the collapse of the marble due to complete evaporation. As the ethanol concentration within the marble is the driving source of the motion we expect that a marble with a larger amount of ethanol will have longer duration of self-locomotion. Figure

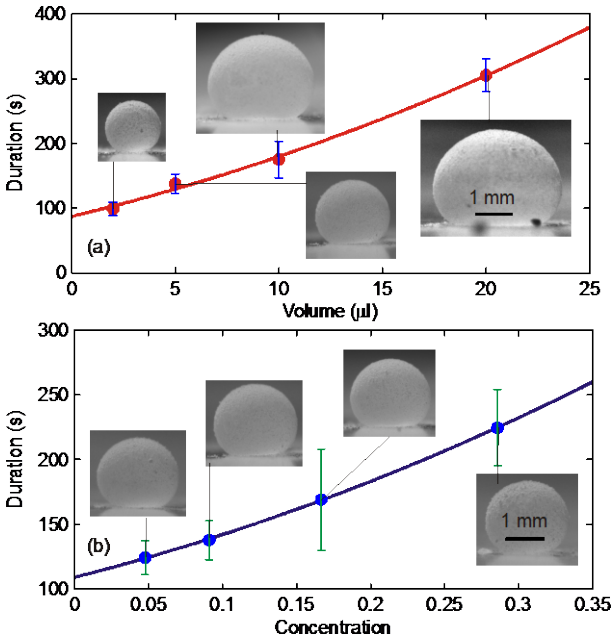

Fig. 5 Duration of the motion as function of volume and concentration: (a) Lifetime of marble motion versus marble volume at a constant volume concentration of ethanol 0.09. The insets show sessile liquid marbles on a solid surface with same volumes and concentrations. (b) Duration of marble motion versus the volume concentration of ethanol at a constant volume of 5 µL. Insets show sessile liquid marble on a solid surface with the same volume and concentrations. Floating ethanol marbles are not shown as they are constantly in motion.

5(a) shows that increasing the volume of the marble increases the lifetime of its motion. Increasing the ethanol concentration at constant volume also increases the amount of ethanol and hence yields a longer lifetime as well.

However, towards the end of the lifetime, the marble motion became less predictable due to its the diminishing driving force. The motion can be interrupted by minute disturbances and may change course or even stop unexpectedly. These minor disturbances include uneven distribution of water surface tension in the vicinity of the marble and the imperfect surface of the container wall. The low ethanol content within the marble, however, is the main reason for the movement stop.

The low level of ethanol was not able to sustain a sufficiently large surface tension difference on the water surface. The ethanol-water mixture started to evaporate even while the marble was being prepared in the powder bed. Thus, the floating marble in the experiment actually has a lower effective ethanol concentration. Preparation, handling and transfer processes were conducted within 30 seconds, smaller than the lifetime of the motion on the order of 100 to 200 seconds. However, some variations are inevitable with the present preparation and handling method.

Conclusion

This paper reports the operational condition of self-driven floating liquid marbles that contain aqueous alcohol solutions. One key parameter was the available free surface of the carrier liquid represented by the ratio between the radii of the bounding ring and the marble R^*. Both the volume concentration of ethanol and the volume of the marble affect this ratio. A marble with higher ethanol concentration can move in smaller rings, but there is a maximum marble volume which any ring can accommodate. The threshold gradient of the surface tension enabling the self-propulsion was estimated. The apparent surface tension of liquid marbles with different volume concentrations of ethanol was measured as well. The motion of the self-driven floating liquid marble was investigated and reported. The kinematic behaviour shows different phases in the lifetime of the marbles. These phases are similar to those mentioned in previous studies on camphor boats. The paper also highlights the present difficulties of a quantitative investigation, but does suggest some scaling laws governing the self-propulsion of liquid marbles. The results show that the lifetime of the motion increases with both marble volume and the concentration of ethanol in the liquid mixtures.

Acknowledgements

We acknowledge Queensland Micro- and Nanotechnology Centre for providing the facilities to make the experiments possible. NTN acknowledges funding support from Griffith University through a start-up grant and a grant from the Griffith University Research Infrastructure Program (GURIP) and the Australian Research Council grant LP150100153.

Notes and references

[a] Queensland Micro- and Nanotechnology Centre, Griffith University, 170 Kessels Road, 4111 Queensland, Australia.
[*] email: nam-trung.nguyen@griffith.edu.au
[b] School of Chemical Engineering, The University of Queensland, Brisbane, Queensland 4072, Australia
[c] Department of Chemical Engineering, University of Newcastle, Callaghan, NSW 2308, Australia
[c] Faculty of Mechanical Engineering, Technion - Israel Institute of Technology, 32000 Haifa, Israel
[d] Ariel University, Chemical Engineering and Biotechnology Department, P.O.B. 3, 40700 Ariel, Israel

† Footnotes should appear here. These might include comments relevant to but not central to the matter under discussion, limited experimental and spectral data, and crystallographic data.
Electronic Supplementary Information (ESI) available: [details of any supplementary information available should be included here]. See DOI: 10.1039/b000000x/

References

1. R.K. Vadivelu, C.H. Ooi, R.Q. Yao, J.T. Velasquez, E. Pastrana, J. Diaz-Nido, F. Lim, J. Ekkberg, N.T. Nguyen, J. St John, *Scientific Reports*, 2015, **5**, 15083.
2. V. Pimienta and C. Antoine, *Curr Opin Colloid In*, 2014, **19**, 290-299.

3. S. Nakata, M. Nagayama, H. Kitahata, N. J. Suematsu and T. Hasegawa, *Physical chemistry chemical physics : PCCP*, 2015, **17**, 10326-10338.
4. Y.-J. Chen, Y. Nagamine and K. Yoshikawa, *Physical Review E*, 2009, **80**, 016303.
5. G. Zhao and M. Pumera, *The Journal of Physical Chemistry B*, 2012, **116**, 10960-10963.
6. T. H. Seah, G. Zhao and M. Pumera, *ChemPlusChem*, 2013, **78**, 395-397.
7. S. Nakata and Y. Hayashima, *Journal of the Chemical Society, Faraday Transactions*, 1998, **94**, 3655-3658.
8. S. Nakata, Y. Iguchi, S. Ose, M. Kuboyama, T. Ishii and K. Yoshikawa, *Langmuir*, 1997, **13**, 4454-4458.
9. S. Nakata, Y. Hayashima and H. Komoto, *Physical Chemistry Chemical Physics*, 2000, **2**, 2395-2399.
10. Y. Hayashima, M. Nagayama and S. Nakata, *The Journal of Physical Chemistry B*, 2001, **105**, 5353-5357.
11. H. Kitahata, S.-i. Hiromatsu, Y. Doi, S. Nakata and M. Rafiqul Islam, *Physical Chemistry Chemical Physics*, 2004, **6**, 2409-2414.
12. R. Sharma, S. T. Chang and O. D. Velev, *Langmuir*, 2012, **28**, 10128-10135.
13. G. Zhao and M. Pumera, *Lab on a Chip*, 2014, **14**, 2818-2823.
14. N. J. Suematsu, T. Sasaki, S. Nakata and H. Kitahata, *Langmuir*, 2014, **30**, 8101-8108.
15. Y. Karasawa, S. Oshima, T. Nomoto, T. Toyota and M. Fujinami, *Chemistry Letters*, 2014, **43**, 1002-1004.
16. S. Oshima, T. Nomoto, T. Toyota and M. Fujinami, *Analytical Sciences*, 2014, **30**, 441-444.
17. E. Bormashenko, Y. Bormashenko, R. Grynyov, H. Aharoni, G. Whyman and B. P. Binks, *The Journal of Physical Chemistry C*, 2015, **119**, 9910-9915.
18. M. I. Newton, D. L. Herbertson, S. J. Elliott, N. J. Shirtcliffe and G. McHale, *Journal of Physics D: Applied Physics*, 2007, **40**, 20-24.
19. Y. Zhao, Z. G. Xu, M. Parhizkar, J. Fang, X. G. Wang and T. Lin, *Microfluid Nanofluid*, 2012, **13**, 555-564.
20. N. T. Nguyen, *Langmuir*, 2013, **29**, 13982-13989.
21. L. Zhang, D. Cha and P. Wang, *Advanced Materials*, 2012, **24**, 4756-4760.
22. Y. Zhao, J. Fang, H. Wang, X. Wang and T. Lin, *Advanced Materials*, 2010, **22**, 707-710.
23. M. Nagayama, S. Nakata, Y. Doi and Y. Hayashima, *Physica D: Nonlinear Phenomena*, 2004, **194**, 151-165.
24. P. Aussillous and D. Quere, *P Roy Soc a-Math Phy*, 2006, **462**, 973-999.
25. E. Bormashenko, A. Musin, G. Whyman, Z. Barkay, A. Starostin, V. Valtsifer and V. Strelnikov, *Colloids and Surfaces A: Physicochemical and Engineering Aspects*, 2013, **425**, 15-23.
26. C. H. Ooi, R. K. Vadivelu, J. St John, D. V. Dao and N.-T. Nguyen, *Soft Matter*, 2015, **11**, 4576-4583.
27. E. Bormashenko, R. Pogreb, G. Whyman, A. Musin, Y. Bormashenko and Z. Barkay, *Langmuir*, 2009, **25**, 1893-1896.
28. T. Arbatan and W. Shen, *Langmuir*, 2011, **27**, 12923-12929.
29. E. Bormashenko, R. Pogreb, G. Whyman and A. Musin, *Colloids and Surfaces A: Physicochemical and Engineering Aspects*, 2009, **351**, 78-82.
30. K. Sefiane, L. Tadrist and M. Douglas, *International Journal of Heat and Mass Transfer*, 2003, **46**, 4527-4534.
31. K. D. O'Hare, P. L. Spedding and J. Grimshaw, *Developments in Chemical Engineering and Mineral Processing*, 2008, **1**, 118-128.